

Estimation of the Impact of Climate Change on Japanese Rice Yield and Water Resources

Shunji Kotsuki

Ph. D. student, Kyoto University, Kyoto 611-0011, Japan. E-mail: kotsuki.shunji.42x@st.kyoto-u.ac.jp

Kenji Tanaka

Associate Professor, Disaster Prevention Research Institute, Kyoto Univ., Kyoto611-0011, Japan.

E-mail: tanaka.kenji.6u@kyoto-u.ac.jp

ABSTRACT: The aim of this study is to estimate the impact of climate change on Japanese rice yield and water resources using a newly-developed Japanese Water Resources Model. The model is composed of five sub-modules: land surface hydrology, irrigation, rice growth, dam operation, and stream flow. Using observed meteorological data for the period of 1994 to 2003, simulated river discharge and rice yields were verified. We estimate impact of climate change on river discharge, rice yields and water stress using bias-corrected outputs from a super high-resolution global climate model under present, near-future, and late 21st century climate conditions. The main findings were as follows: (1) Simulated rice yield and river discharge using observed meteorological forcings have shown good agreement with statistical data. The snowfall correction and the dam operation module clearly improve the simulated river discharge. (2) The seasonal discharge will change dramatically, especially at the end of the 21st century, in basins facing the Sea of Japan that currently experience heavy snowfall. A depletion of annual snowfall would be result from the warming temperature trend in many basins. (3) Climate change is predicted to strengthen the water stress in many basins in the northeastern Japan, which uses large amounts of snowmelt water to prepare rice paddies for planting. Water stress would also increase in small basins. (4) Climate change may mitigate low-temperature stress and expand the arable area, including into high-mountain areas and northern prefectures. Many prefectures facing the Sea of Japan are predicted to experience decrease in rice yield. The simulation clearly demonstrates the regions that should consider changing the period of cultivation to mitigate the decrease in rice yields and increased water stress.

KEY WORDS: Climate change, Water resources model, Japanese river, Rice yield, human activity

1 INTRODUCTION

As the problems associated with climate change increase, evaluations of the likely impacts are urgently required, such as by climatological and hydrological modeling. The performance of general circulation models (GCMs) has improved, and GCM outputs have been used in hydrological models to assess the impacts of climate change. While many impact assessment studies for Japan using GCM outputs have been reported, many have focused on a particular basin (e.g., Sato *et al.*, 2011; Kim *et al.*, 2011). Few impact assessment studies have covered the entire Japanese basin area to identify areas vulnerable to climate change. The few previous studies that have examined all of Japan have assessed climate change impacts on seasonal discharge, flood risk, and flood damage (Kazama *et al.*, 2009; Tachikawa *et al.*, 2010), but none has investigated the water demand and supply balance. We developed the novel Japanese Water Resources Model to assess the impact of climate change on seasonal discharge, water demand-supply balances, and rice yield. This paper describes the validation of our model using meteorological forcing with observed data and the impact of climate change on Japanese water resources, estimated using bias-corrected GCM outputs.

2 METHODOLOGY

2.1 The Japanese Water Resources Model

The Japanese Water Resources Model proposed in this paper is composed of five sub-modules: land surface hydrology, irrigation, rice growth, dam operation, and stream flow (Figure 1). The model has the advantage of simulating not only the natural water cycle on land but also rice yields and the effects of human activities such as dam operations, water withdrawal, and irrigation.

The rice growth module was developed from a field-scale model, the Simulation Model for Rice-Weather Relationship (SIMRIW; Horie *et al.*, 1995, Iizumi *et al.*, 2009). Using temperature and short-wave radiation as input data, the module simulates rice growth and rice yields by considering high-temperature and low-temperature stresses on yield. The model parameters were originally at the field scale for specific cultivars, but prefecture-specific parameters were optimized in the present study using particle swarm optimization (PSO; Kennedy and Eberhart, 1995).

The land surface module calculates the energy, radiation, and water budgets on the land surface with seven meteorological forcings: temperature, specific humidity, short-wave radiation, long-wave radiation, atmospheric pressure, wind speed, and precipitation. In this study, the Simple Biosphere Model including Urban Canopy (SiBUC; Tanaka, 2004) was used to calculate the land surface process.

The basic function of the irrigation module is to maintain the water level in paddy fields and soil moisture in croplands within an appropriate range that is defined for each growing stage. The water level in paddy fields and soil moisture in croplands are calculated in the land surface module. The crop calendar, which defines the planting date and harvesting date, is specified by the rice growth module.

The stream process calculates the river discharge using runoff calculated by the land surface process. The river discharge is simulated with a kinematic wave equation. Intakes and drainages for agricultural, domestic, and industrial water usage are considered in this process.

The dam operation module was developed to include the effect of 1,231 Japanese dams with volumes over 100,000 m³. After classifying each dam's objective into three types (flood protection, water utilization, and multi-objective), the dam operation can be briefly described by the following equations:

$$Q_{base} = \begin{cases} Q_{flood} \\ Q_{norm} \end{cases} \text{ when } \begin{cases} Q_{inf} > Q_{flood} \\ Q_{inf} \leq Q_{flood} \end{cases} \quad (1)$$

$$Q_{ouf} = \max \{ Q_{base}, \beta \cdot Q_{req} \} \quad (2)$$

where Q_{inf} is inflow [m³s⁻¹], Q_{ouf} is terminal outflow [m³s⁻¹], Q_{norm} is the maintenance outflow [m³s⁻¹], Q_{base} is the basic outflow [m³s⁻¹], Q_{flood} is the outflow during a flood [m³s⁻¹], and Q_{req} is the outflow requirement from downstream [m³s⁻¹]. The outflow coefficient for requirement β was set as 2.5 in this study. Equation (1) describes operations for flood protection and equation (2) describes operations for water utilization, respectively. The maintenance outflow Q_{norm} is determined from the following equations according to the objective of each dam:

$$Q_{norm,f} = \min \{ Q_{flood}, Q_{inf} \} \quad (3)$$

$$Q_{norm,u} = \begin{cases} Q_{low} & \text{for rainy season} \\ Q_{dry} & \text{for dry season} \end{cases} \quad (4)$$

$$Q_{norm,m} = \begin{cases} Q_{norm,f} & \text{for } St > V_u \\ Q_{norm,u} & \text{for } St \leq V_u \end{cases} \quad (5)$$

where Q_{low} is low-water outflow [m³s⁻¹], Q_{dry} is outflow during the dry season [m³s⁻¹], V_u is the capacity of the dam [m³], and St is the storage of dam. The subscripts f , u and m indicate a flood protection dam, a

water utilization dam, and a multi-objective dam, respectively. The outflow during the dry season Q_{dry} , which is determined at the end of each rainy season, is calculated by the storage divided by the period until the next rainy season. Following a river discharge analysis from 1994 to 2003 without dams, the rainy season was determined for each dam as the period when the mean discharge of the month was greater than the annual average discharge. Using the daily-discharge duration curve from the 10-year simulation without the dam module, the 5% and 50% percentile values were set as the outflow during a flood Q_{flood} and the low-water outflow Q_{low} , respectively.

2.2 Data sets

The meteorological forcing, statistical, and geophysical data used in this study are shown in **Tables 1** and **2**. Precipitation data were corrected using the following equation because precipitation gauge measurements underestimate snowfall (Yang *et al.*, 1998):

$$CR = 1 / (1 + 0.231 \cdot Ws) \quad \text{when} \{T < T_c\}, \quad T_c = 11.01 - 1.5e \quad (6)$$

where CR is the gauge catch ratio [-], Ws is wind speed [ms^{-1}], T is surface temperature [K], e is surface vapor pressure, and T_c is critical temperature [K].

2.3 Validation using observed forcing

Using observed meteorological data for the period of 1994 to 2003, simulated river discharge and rice yields were validated. Model errors were calculated with the following equations:

$$BL = \frac{\bar{V}_s - \bar{V}_o}{\bar{V}_o}, \quad MRE = \frac{1}{N} \sum \frac{|V_s - V_o|}{V_o}, \quad RMSE = \sqrt{\frac{1}{N} \sum (V_s - V_o)^2}, \quad Nash = 1 - \frac{\sum (V_s - V_o)^2}{\sum (\bar{V}_o - V_o)^2} \quad (7)$$

where V_s is the simulated value and V_o is the observed value.

2.3.1 Validation of the rice growth module

A comparison of the heading dates, harvesting dates, and yield simulated by our model and reported by Iizumi *et al.* (2009) is shown in Table 3. ‘‘North pref.’’ signifies the averaged results for the northern prefectures (Hokkaido and Tohoku District). ‘‘South pref.’’ signifies the averaged results for the southern prefectures (Kyushu and Shikoku District). Although our parameter identification method was different from that used by Iizumi *et al.*, (2009), computed errors were almost the same, suggesting that the parameters of the rice growth module were identified correctly. Comparisons of statistical and simulated rice yield from 1991 to 2004 in the north, east, middle, and west regions of Japan are shown in Figures (b-1), (b-2), (b-3), and (b-4). The simulated yields agreed well with the statistical data and reflected the damage resulting from a cold summer in 1993.

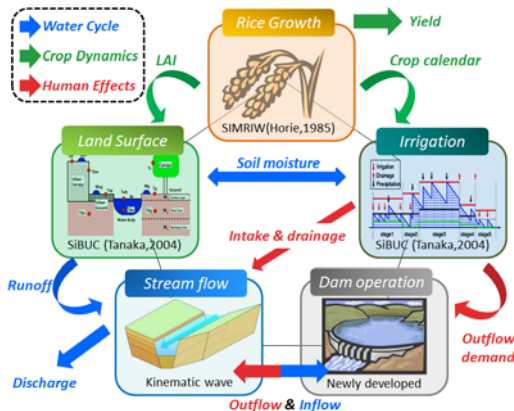


Figure 1 Schematic diagram of the Japanese Water Resources Model used for this study. The model comprises five sub-modules: rice growth, hydrological land surface, irrigation, stream flow, and dam operation.

Table 1 Meteorological forcing data sets

Observed precipitation	Kamiguchi <i>et al.</i> , 2010
Observed other forcing	JMA, AMeDAS
MRI-AGCM20	Kusunoki <i>et al.</i> , 2011

JMA: Japan Meteorological Agency

AMeDAS: Automated Meteorological Data Acquisition System

Table 2 Geophysical and statistical data sets

Flow direction	Global Drainage Basin Database (GDBD; Masutomi <i>et al.</i> , 2009)
Channel slope	
Soil Physical	Ecoclimap ver.1 (Meteo-France)
NDVI	Spot Vegetation 1km
Population	National Land Numerical Information download service http://nlftp.mlit.go.jp/ksj-e/index.html
Dam	
Water usage	
Land cover	

Table 3 Comparison of heading dates, harvesting dates, and yield simulated by our model and Iizumi *et al.*, (2009)

		Heading dates [day]		Harvesting dates [day]		Rice Yield [t/ha]	
		North pref.	South pref.	North pref.	South pref.	North pref.	South pref.
This study	R ²	0.807	0.459	0.860	0.347	0.607	0.552
	RMSE	1.3	1.5	1.7	1.9	0.45	0.36
Iizumi (2009)	R ²	0.817	0.435	-	-	0.518	0.417
	RMSE	2.3	3.2	-	-	0.49	0.36

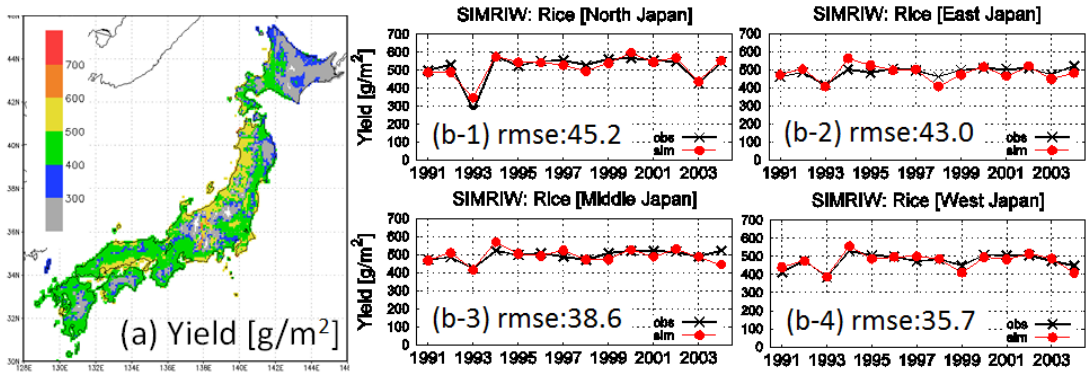


Figure 2 Distribution of potential rice yield using observed forcing (a). Comparisons of statistical and simulated rice yield from 1991 to 2004 in north, east, middle, and west regions of Japan are shown in Figure (b-1), (b-2), (b-3) and (b-4). Black lines and red lines respectively show statistical and simulated rice yield. [unit: g/m²]

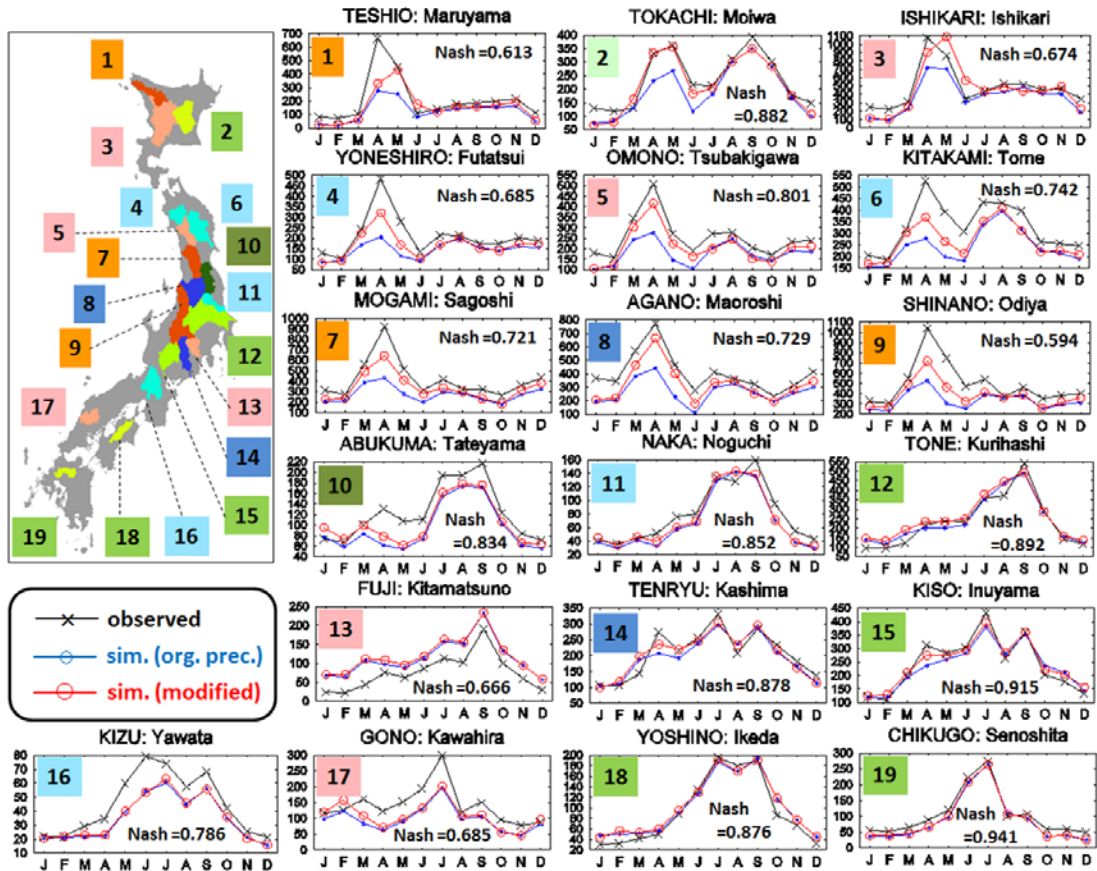


Figure 3 Seasonal validation of the monthly river discharge at major 19 first-grade rivers in Japan [unit: m³s⁻¹]. Black lines with X-marks, blue lines with circles, and red lines with circles respectively represent observed discharge, simulated discharge without and with correction of snowfall data.

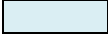
2.3.2 Validation of river discharge

A seasonal validation of the monthly river discharge at 19 major first-grade rivers in Japan is shown in Figure 3. The Nash-Sutcliffe model efficiency coefficient (hereafter Nash) exceeds 0.8 in most rivers, suggesting that our water resources model reproduced the seasonal discharge well. The effect of a snowfall correction is reflected in the difference between the blue (without correction) and red (with correction) lines in Figure 3. The snowfall corrections clearly improve the simulated river discharge during the snow melt season from March to June in northern Japanese rivers. The periods of snowmelt are also reproduced in Figure 3, suggesting that accumulation and melting processes of snow on land surface are calculated correctly in our Water Resources Model.

Water balance error and mean relative error were calculated for the 19 river stations to verify the effects of snowfall correction and the dam operation module (Table 3-a). NS, SC, DA, and ND in the table are the mean values with no snowfall correction, snowfall correction, no dam, and dam operation, respectively. Blue and green labels in the table show the improvement of the simulation following the snowfall correction and the dam operation module, respectively. Water balance error was improved for most stations following the snowfall correction. Seasonal river discharge was also improved by the dam operation module. Clearly, the module describes the dam operation correctly. Actual dam operations have to be used for simulations in specific river basins.

Table 3 Results at gauging stations of 19 major rivers of (a) validation using observed forcing, and (b) estimated impact of climate change on river discharge using GCM output. Water balance error (BL) and mean relative error (MRE) were calculated to verify effects of snowfall correction and the dam operation module in table 3-a. Water balance error (BL) and Nash-Sutcliffe model efficiency coefficient (Nash) were calculated to estimate impact of climate change on river discharge. NS, SC, DA, ND respectively represent simulations without the snowfall correction, with the snowfall correction, without the dam module, and with the dam module. Blue and green labels in the table show the improvement of the simulation following the snowfall correction and the dam operation module, respectively. Light and dark red colors show change and dramatic change in annual river discharge and seasonal discharge.

Climate	Error function	(a) Validation using observed forcing				(b) Impact estimation			
		Present (1994 - 2003)				Future1		Future2	
		BL		MRE		BL	Nash	BL	Nash
Model	NS,DA	SC,DA	SC,ND	SC,DA	SC, DA				
1	Teshio	-39.6	-24.5	0.385	0.362	+ 7.8	0.944	+12.7	0.650
2	Tokachi	-19.3	- 8.1	0.235	0.198	+ 0.6	0.974	+11.1	0.871
3	Ishikari	-23.0	- 4.0	0.335	0.291	+ 9.2	0.950	+17.3	0.783
4	Yoneshiro	-31.6	-20.9	0.235	0.226	- 0.2	0.676	+ 9.2	-0.131
5	Omono	-30.1	-18.4	0.215	0.205	+ 5.6	0.477	+ 9.4	-0.455
6	Kitakami	-26.8	-18.8	0.199	0.195	+ 2.3	0.738	+ 5.3	0.433
7	Mogami	-34.4	-19.8	0.197	0.196	+ 6.5	0.554	+ 7.0	-0.961
8	Agano	-34.4	-19.8	0.238	0.231	+ 5.8	0.745	+ 3.1	-0.116
9	Shinano	-33.3	-22.0	0.214	0.203	+ 4.3	0.797	+ 5.9	-0.348
10	Abukuma	-23.1	-16.0	0.282	0.261	+ 6.0	0.911	- 5.6	0.735
11	Naka	-14.5	-9.6	0.256	0.249	+ 7.5	0.890	- 0.3	0.804
12	Tone	+ 1.8	+ 9.7	0.269	0.282	+ 4.6	0.908	+ 6.1	0.803
13	Fuji	+49.1	+56.9	1.263	1.290	+ 2.8	0.934	+ 4.9	0.921
14	Tenryu	- 6.2	- 1.3	0.207	0.237	+ 3.5	0.955	+ 4.5	0.932
15	Kiso	- 3.6	+ 1.1	0.152	0.185	+ 1.9	0.975	- 1.1	0.852
16	Kizu	-23.8	-21.7	0.306	0.275	+ 4.3	0.781	+ 5.9	0.673
17	Gono	-31.5	-23.1	0.354	0.323	+ 2.5	0.722	+13.6	0.307
18	Yoshino	+ 6.2	+ 9.3	0.406	0.483	- 1.1	0.933	+ 1.2	0.957
19	Chikugo	-17.2	-15.2	0.282	0.267	-17.0	0.693	- 1.3	0.787

 : improvement with snowfall correction
 : improvement with dam operation

 : change caused by climate change
 : dramatic change caused by climate change

3 ESTIMATION OF THE IMPACT OF CLIMATE CHANGE

3.1 Bias correction of GCM data

The impacts of climate change on river discharge, rice yields, and water stress were estimated using the forcing outputs from a super high-resolution global climate model, the Japan Meteorological Research Institute atmospheric general circulation model with 20-km resolution (MRI-AGCM20; Kusunoki *et al.*, 2011) under present (from 1979 to 2003), near future (from 2015 to 2039, hereafter future1), and late 21st century (from 2075 to 2099, hereafter future2) conditions. Bias correction was undertaken for seven meteorological forcings using observed data with the following equation:

$$F_{y,m,d,h}(x,y) = F_{y,m,d,h}^{GCM}(x,y) + (\bar{F}_{present,m,riv(x,y)}^{obs} - \bar{F}_{present,m,riv(x,y)}^{GCM}) \quad (8)$$

where F is the corrected forcing, F^{obs} is the observed forcing, F^{GCM} is the forcing from the GCM, and $\bar{F}_{present}$ is the mean forcing from 1991 to 2004. The subscripts y , m , d , and h represent year, month, day and hour, and $riv(x,y)$ is river basin which each mesh belongs to.

3.2 Effects on water resources

Water balance error and Nash were calculated to estimate the impact of climate change on river discharge (Table 3-b). The spatial distribution of Nash in Japanese basins is shown in Figure 4-a. The table and figure suggest that the seasonal discharge will change dramatically, especially at the end of the 21st century, in basins facing the Sea of Japan that currently experience heavy snowfall. Changes in annual snowfall are shown in Figure 4-b, which indicates that a depletion of annual snowfall would result from the warming temperature trend in many basins. A depletion of snowfall would increase the winter discharge and decrease the spring discharge.

The cumulative withdrawal to demand ratio (CWD; Hanasaki *et al.*, 2008) was calculated to evaluate the impact of changes in seasonal discharge on the water demand and supply balance. CWD water stress in Japanese basins was calculated by the following equations:

$$CWD_i = 100 \cdot \sum \omega_{week,i} / \sum D_{week,i} \quad (9)$$

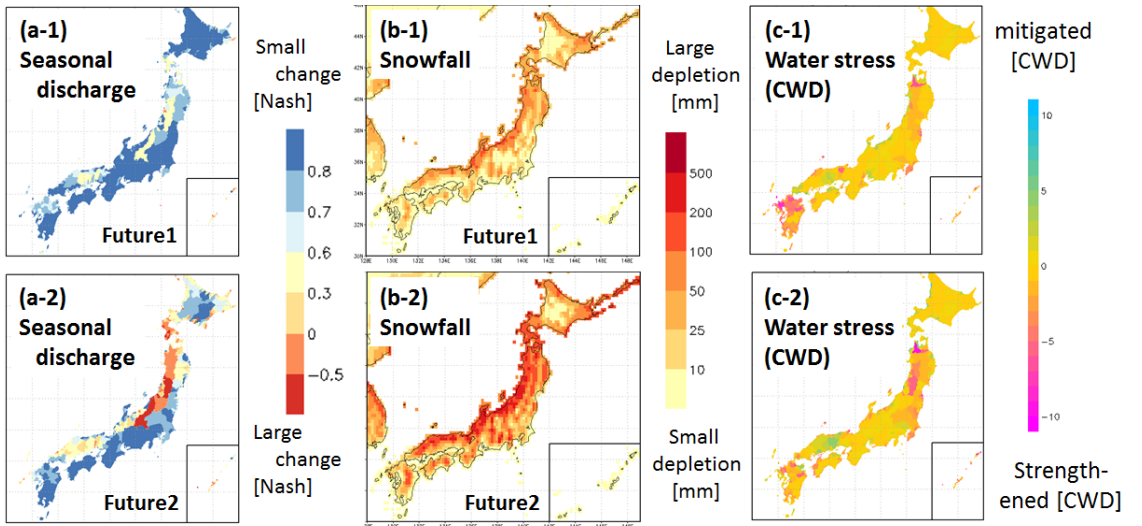


Figure 4 Changes in (a) seasonal discharge, (b) annual snowfall, and (c) the CWD water stress caused by climate change. Figure (a-1), (b-1) and (c-1) show difference between near future climate (2015 – 2039) and present climate (1979 – 2003). Figure (a-2), (b-2) and (c-2) show difference between end of 21th century climate (2075 – 2099) and present climate. Changes in seasonal discharge were estimated by calculating Nash-Sutcliffe model efficiency coefficient using averaged monthly discharge under the three climate conditions.

$$\omega_{week,i} = \begin{cases} D_{week,i} \\ Q_{week,i} \end{cases} \text{ when } \begin{cases} Q_{week,i} \geq D_{week,i} \\ else \end{cases} \quad (10)$$

where ω_{week} is the weekly water intake [$m^3/week$], D_{week} is the weekly water demand [$m^3/week$], and Q_{week} is the weekly water supply [$m^3/week$]. Agricultural, industrial, and domestic water demands were also included.

Changes in the CDW water stress are shown in Figure 4-c. Cold and warm colors represent the mean mitigated and strengthened water stresses caused by climate change, respectively. Climate change is predicted to strengthen the water stress in many basins in the northeastern Japan (the Tohoku District). Because the Tohoku District uses large amounts of snowmelt water to prepare rice paddies for planting, a decrease in the spring discharge would increase water stress in this district. Water stress would also increase in small basins, as shown in Figure 4-c. Rainfall intensity is predicted to increase due to the warm temperature trends under future climate change. Thus, water stresses would also be strengthened in basins that do not have large reservoirs. It is clear that many Japanese basins will face severe challenges in water resource management under future climate scenarios.

3.3 Effects on rice yields

Changes in rice yield, absorbed short-wave radiation after the flowering stage, and low temperature stresses on yields are shown in Figures 5-a, 5-b, and 5c. The hatches in Figure 5 indicate regions incompatible with farming under present climate conditions because of cold temperatures. Regions with hatches are predicted to experience dramatic increases in rice yield, implying that climate change may have the benefit of expanding the arable area, including into high-mountain areas and northern prefectures. Figure 5-a indicates that rice yields will increase in many prefectures under future climate change conditions. Regions where a decrease in rice yield is predicted correspond to those regions where decreasing amounts of short-wave radiation are absorbed. A change in the timing of autumn rain may decrease the amount of short-wave radiation absorbed. Many prefectures facing the Sea of Japan are predicted to experience such a decrease in rice yield and absorbed short-wave radiation. Those prefectures are also predicted to experience a dramatic change in seasonal river discharge. Prefectures facing the Sea of Japan should consider changing the period of cultivation to mitigate the decrease in rice yields and increased water stress. However, low-temperature stresses would be mitigated by the warming temperature trend shown in **Figure 5-c**. Damage during cold summers in northern prefectures would be mitigated under future climate change conditions.

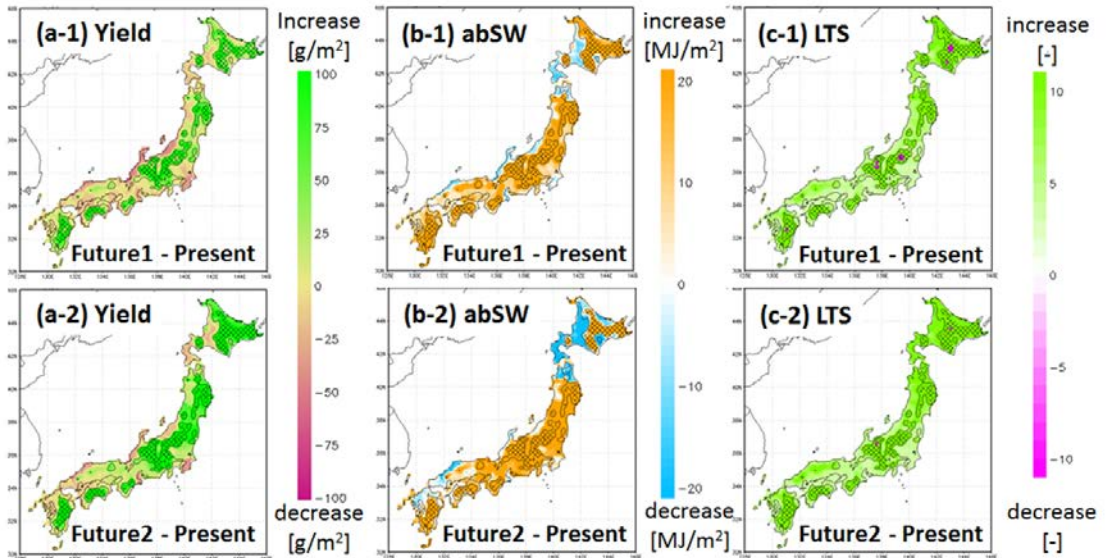


Figure 5 Changes in (a) rice yield, (b) absorbed short-wave radiation (abSW) after flowering stage, and (c) low temperature stresses (LTS) for yield. The hatches in the figures indicate aregions incompatible with farming under present climate condition because of cold temperature.

4 CONCLUSIONS

In this study, we newly developed the Japanese Water Resources Model to assess the impact of climate change on seasonal discharge, water balances, and rice yield. This paper has described the validation of our model using observed meteorological forcings and the impact of climate change on Japanese water resources using GCM outputs. The main findings were as follows:

- 1) Simulated rice yield and river discharge using observed meteorological forcings have shown good agreement with statistical data. The snowfall correction and the dam operation module clearly improve the simulated river discharge.
- 2) The seasonal discharge will change dramatically, especially at the end of the 21st century, in basins facing the Sea of Japan that currently experience heavy snowfall. A depletion of annual snowfall would be result from the warming temperature trend in many basins.
- 3) Climate change is predicted to strengthen the water stress in many basins in the Tohoku District located in the northeastern Japan. Because the Tohoku District uses large amounts of snowmelt water to prepare rice paddies for planting, a decrease in the spring discharge would increase water stress in this district. Water stress would also increase in small basins. It is clear that many Japanese basins will face severe challenges in water resource management under future climate scenarios.
- 4) Climate change may mitigate low-temperature stress and expand the arable area, including into high-mountain areas and northern prefectures. Many prefectures facing the Sea of Japan are predicted to experience decrease in rice yield caused by depletion of the absorbed short-wave radiation. Prefectures facing the Sea of Japan should consider changing the period of cultivation to mitigate the decrease in rice yields and increased water stress.

ACKNOWLEDGEMENT

This work was conducted as a part of the SOUSEI program funded by the Ministry of Education, Culture, Sports, Science and Technology (MEXT), Japan. This study was also supported by the Japan Society for the promotion of Science (JSPS).

References

- Hanasaki N, Kanae S, Oki T, Masuda K, Motoya K, Shirakawa N, Shen Y, Tanaka K. 2008. An integrated model for the assessment of global water resources—part 2: applications and assessments. *Hydrology and Earth System Sciences* 12: 1027-1037. doi: 10.5194/hess-12-1027-2008.
- Horie T, Nakagawa H, Centeno H.G.S., Kropff M, 1995. The rice crop simulation model SIMRIW and its testing, In *Modeling the Impact of Climate Change on Rice in Asia*, CAB International, Oxon: pp.51-66 (UK).
- Iizumi T, Yokozawa M, Nishimori M. 2009. Parameter estimation and uncertainty analysis of large-scale crop model for paddy rice: Application of a Bayesian approach. *Agricultural and forest meteorology*, 149: 333-348.
- Kamiguchi K, Arakawa O, Kitoh A, Hamada A, Yasutomi N. 2010. Development of APHRO_JP, the first Japanese high-resolution daily precipitation product for more than 100 years. *Hydrological Research Letters* 4: 60-64.
- Kazama S, Sato A, Kawagoe S. 2009. Evaluating the cost of flood damage based on changes in extreme rainfall in Japan, *Sustainability Science*, Vol.4, Iss.1, 61-69.
- Kennedy J, and Eberhart R. 1995. Particle Swarm Optimization, *Proceedings of IEEE International Conference on Neural Networks*, 1942-1948.
- Kim S, Tachikawa Y, Nakakita E, Yorozu K, Shiiba M. 2011. Climate change impact on river flow of the tone river basin, Japan. *Journal of Japan Society of Civil Engineers, Ser. B1* Vol67-4: 85-90.
- Kusunoki S, Mizuta R, Matsueda M. 2011. Future changes in the East Asian rain band projected by global atmospheric models with 20-km and 60-km grid size. *Climate Dynamics* 37: 2481-2493. doi: 10.1007/s00382-011-1000-x.
- Masutomi Y, Inui Y, Takahashi K, Matsuoka Y. 2009. Development of highly accurate global polygonal drainage basin data. *Hydrological Processes* 23: 572-584. doi:10.1002/hyp.7186.
- Sato Y, Kojiri T, Michihiro Y, Suzuki Y, Nakakita E. 2011. Analysis of extreme hydrological events in major river basins in Japan under climate change. *Proceedings of 2011 IAHR World Congress*: 710-717.
- Tachikawa Y, Takino S, Fujioka Y, Yorozu Y, Kim S, Shiiba S. 2010. Projection of river discharge of Japanese river basins under climate change scenario, *Proc. of the 5th Conference of Asia Pacific Association of Hydrology and Water Resources (APHW)*: 139-145.
- Tanaka K. 2004. Development of the New Land Surface Scheme SiBUC Commonly Applicable to Basin Water Management and Numerical Weather Prediction Model. *Doctoral Dissertation, Graduate School of Engineering, Kyoto University*: Kyoto; 289.
- Yang D, Barry Y, Goodison, Metcalfe J, 1998. Accuracy of NWS 8" standard non-recording precipitation gauge: Result and application of WMO intercomparison. *Journal of Atmospheric and Oceanic Technology*, 15: 54-68.